32040 (1996)]. Such a sequence should show the appearance of a tagged D or DD residue at the reducing end. However, we find all the different experiments used in the elucidation of the decasaccharide sequence to be consistent with each other in the appearance of a 4-7 tagged product and not a D (or a DD) product. This saccharide does not contain an intact AT-III binding site, as proposed. Therefore, we sought confirmation of our proposed sequence through the use of integral glycan sequencing (IGS), which agreed with our analysis.

15. DCMPs are found in dense connective tissues such as bone and cartilage. The basic repeat unit of DCMP can be represented as $-(\beta\ 1\rightarrow4)\ U_{2X}-(\alpha/\beta\ 1\rightarrow3)\ Gal_{NAc,4X,6X}-$, where U is uronic acid, Gal_{NAc} is a *N*-acetylated galactosamine, and there are 16 disaccharide building blocks for DCMP. Like the heparinases that degrade HLGAGs, there are distinct chondroitinases and other chemical methods available that clip at specific glycosidic linkages of DCMP and serve as experimental constraints. Furthermore, because DCMPs are acidic polysaccharides, the MALDI-MS techniques and methods used for HLGAGs can be readily extended to the DCMPs.
16. The monomeric units of NAN and NGN are linked by α 2-8 glycosidic linkages and can be modified at the 4-O, 7-O, and 9-O positions. Methods of purifying and characterizing PSA oligosaccharides using high-performance liquid chromatography, CE, and MS have very recently been established. In addition, chemical and exosialydases and endosialydases that cleave at distinct glycosidic linkage of PSA are available and can serve as experimental constraints.
17. The sequencing approach presently uses a brute force method because many of the rules regarding the specificity of enzymes that degrade and modify complex polysaccharides are in the developmental stage. Once these rules or constraints are fully developed, more intelligent algorithms such as a genetic algorithm or Monte Carlo optimization could be used to search a much narrower search space for the correct sequence. The combination of more efficient constraints and algorithms will thus lead to a fully automated sequencing approach.
18. The use of heparinases was essentially as described in references in (*11*). Digests were designated as either short or exhaustive. Short digests were completed with 50 nM enzyme for 10 min. Exhaustive digests were completed with 200 nM enzyme for either 4 hours or overnight. Partial nitrous acid cleavage was completed using a modification of published procedures. Briefly, to an aqueous solution of saccharide was added a 2× solution of sodium nitrite in HCl so that the concentration of nitrous acid was 2 mM and that of HCl was 20 mM. The reaction was allowed to proceed at room temperature with quenching of aliquots at various time points through the addition of 1 μl of 200 mM sodium acetate and of bovine serum albumin (1 mg/ml; pH 6.0). Exhaustive nitrous acid cleavage was completed by reacting saccharide with 4 mM nitrous acid in HCl overnight at room temperature. In both cases, it was found that the products of nitrous acid cleavage could be sampled directly by MALDI without further cleanup and without the need to reduce the anhydromannose residues to anhydromannitol. The entire panel of HLGAG-degrading exoenzymes was purchased from Oxford Glycosystems (Wakefield, MA) and used as suggested by the manufacturer.
19. G. Venkataraman *et al.*, *Proc. Natl. Acad. Sci. U.S.A.* **96**, 1892 (1999).
20. Supported in part by the Massachusetts Institute of Technology and NIH (grant number GM 57073). We thank K. Biemann for help and input on the MALDI-MS; K. Pojasek for technical help with MS; R. Linhardt and J. Turnbull for saccharides and corroboration of our AT-III decasaccharide microsequencing results with exoenzyme sequencing (IGS); and J. Essigmann, A. Grodzinsky, R. Langer, and V. Sasisekharan for critical comments.

26 May 1999; accepted 1 September 1999

Stability and Variability in Competitive Communities

A. R. Ives,* K. Gross, J. L. Klug

Long-term variability in the abundance of populations depends on the sensitivity of species to environmental fluctuations and the amplification of environmental fluctuations by interactions among species. Although competitive interactions and species number may have diverse effects on variability measured at the individual species level, a combination of theoretical analyses shows that these factors have no effect on variability measured at the community level. Therefore, biodiversity may increase community stability by promoting diversity among species in their responses to environmental fluctuations, but increasing the number and strength of competitive interactions has little effect.

The stability of an ecological community is thought to depend on the number of species it contains and the strengths of interactions between them (*1*). Stability also depends on the organizational level at which it is measured. In model ecosystems, May (*2*) showed that increasing the strength and number of species interactions decreases the stability of individual species' dynamics. In contrast, experimental studies (*3*) showed that large communities of plant competitors may be more stable than small communities when stability is measured in terms of the total biomass of all species.

The stability of ecological communities is commonly characterized by one of five properties: mathematical stability, resilience, resistance, persistence of species, and variability (*4*). Of these, variability is the most frequently measured, yet least understood from a theoretical perspective. Our analyses address the effects of interspecific competition and species diversity on variability in the biomass of individual species and variability in total community biomass. Environmental fluctuations cause short-term (year-to-year) changes in species biomasses. Species interactions then act as a filter through which short-term environmental variability is translated into long-term variability in biomass. Here, we ask how this filter is affected by the strength of species interactions and the number of species in a community. We use an analytical approximation to derive general predictions, and explicit numerical models for quantitative illustration.

The general form of the systems we consider is

$$x_i(t+1) = x_i(t)\,F\left[x_i(t), \sum_{j\neq i}^{n} \alpha_{ij}x_j(t), \varepsilon_i(t), r_i, K_i\right] \quad (1)$$

where $x_i(t)$ is the biomass of species i in year t; $F[\ ]$ is a function giving the change in biomass between years; r_i and K_i are the species-specific intrinsic rate of increase and carrying capacity, respectively; and α_{ij} is the competition coefficient measuring the effect of species j on species i. The model is parameterized so that, in the absence of environmental variability, when $r_i > 1$, populations show overcompensating dynamics, and when $r_i < 1$, biomasses tend to approach equilibrium monotonically. Environmental fluctuations are included with species-specific random variables $\varepsilon_i(t)$. To account for similarities among species in their responses to environmental fluctuations, we assume that the $\varepsilon_i(t)$ values are correlated with correlation coefficient ρ.

We measure variability at two levels. For the species level, we use the sum of the variances of the biomasses of constituent species, $V_n^s = \Sigma_{i=1}^{n} V[x_i(t)]$, where n is the number of species in the community. For the community level, we consider the variance of the aggregate biomass in the community, $V_n^c = V[\Sigma_{i=1}^{n} x_i(t)]$. Measuring variability in this way relates our results directly to experimental studies employing variances (*3–5*).

Analytical approaches provide general conclusions that are independent of detailed model assumptions. Although variances in species biomasses produced by Eq. 1 depend on nonlinearities in $F[\ ]$, variances can be approximated with the first-order autoregression model (*6*)

$$\mathbf{X}(t+1) = \mathbf{C}\mathbf{X}(t) + \mathbf{E}(t) \quad (2)$$

where $\mathbf{X}(t)$ is a vector of species biomasses $\Delta x_i(t)$ relative to the mean [$\Delta x_i(t) = x_i(t) - \bar{x}$] and $\mathbf{E}(t)$ is a vector of random variables that contains the environmentally driven changes in species biomasses from one year to the

Department of Zoology, University of Wisconsin-Madison, Madison, WI 53706, USA.

*To whom correspondence should be addressed. E-mail: arives@facstaff.wisc.edu

next. Matrix **C** gives interaction strengths among species and is analogous to the community matrix used in deterministic stability analyses.

The short-term changes in biomass, given by $\mathbf{E}(t)$, are amplified through **C** to give the variance in long-term biomass. Specifically, the eigenvectors of **C** give new axes for the n-dimensional space of species biomasses, and along each axis w_k, the variance in biomasses V_k, and the environmental variance U_k, are related by (*6, 7*)

$$V_k = \frac{U_k}{1 - \lambda_k^2} \quad (3)$$

where λ_k is the eigenvalue corresponding to w_k (Fig. 1A). λ_k is constrained to have a magnitude of <1 for stable systems. The larger the magnitude of λ_k, the greater the amplification of environmentally driven variance U_k and hence the greater the variance in species biomass V_k. Values of λ_k depend on the structure of **C** and therefore reveal how the strength and number of species interactions affect variance in species biomass.

An informative special case arises when all species have the same values of r_i, K_i, and α_{ij}. In this case, one eigenvalue $\lambda_1 = 1 - r$, with corresponding eigenvector $w_1 = [1, 1, \ldots, 1]$. For all other $n - 1$ eigenvalues (*8*)

$$\lambda_k = 1 - r\left[\frac{n - 1 - \alpha}{(n - 1)(\alpha + 1)}\right] \quad (4)$$

with corresponding eigenvectors perpendicular to w_1. Three results follow. First, the community-level variance in biomass, $V_n^c = V[\sum_{i=1}^n x_i(t)]$, is independent of the strength of competition among species, α, and the number of species, n. This is because the sum of species biomasses is proportional to the projection of species biomasses onto $w_1 = [1, 1, \ldots, 1]$, and amplification of variances along w_1 is governed only by $\lambda_1 = 1 - r$. Second, the species-level variance in biomass, $V_n^s = \sum_{i=1}^n V[x_i(t)]$, may either increase or decrease with α and n. λ_k ($k \neq 1$, Eq. 4) increases with α and decreases with n. Therefore, when $\lambda_k > 0$, increasing α or decreasing n increases λ_k^2, thereby increasing the amplification of environmentally driven variability and increasing species-level variances. When $\lambda_k < 0$, increasing α or decreasing n initially decreases λ_k^2 but then increases λ_k^2 if λ_k becomes positive. Thus, amplification of species-level variance first decreases but then may increase. Third, the effects of changing α and n on species-level variances are reduced by positive environmental correlation; in the extreme case of $\rho \to 1$, species biomasses lie along w_1, so their variance is determined by λ_1, which is independent of α and n.

The analytical results are based on a linear approximation. Nonetheless, numerical studies show that the results hold approximately for nonlinear systems. For illustration, we use Lotka-Volterra competition equations to construct two contrasting models with (model A) and without (model B) interspecific competition (*9*). We keep mean total biomass the same for both communities, allowing us to compare variances directly. In model A, we assume that α is the same for all interspecific interactions.

For both models, increasing the strength of competition (either intra- or interspecific) reduces biomass, so we display results in terms of the reduction in total community biomass (Fig. 2). Species-level and community-level variances decrease as mean biomass decreases, because variances scale with the square of the mean. The important biological patterns that correspond to the analytical results are in the comparisons between models A (Fig. 2, solid lines) and B (Fig. 2, dashed lines).

Community-level variances are almost identical for both models (Fig. 2), indicating that interspecific competition has little influence on community-level variances. When interspecific competition creates negative covariances between species, it also increases species-level variances (Fig.

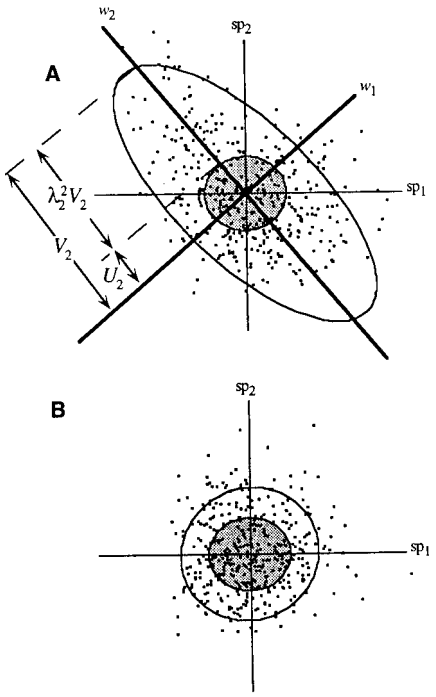

Fig. 1. Joint distributions of competitors (sp_1 and sp_2) in a two-species community in the (**A**) presence (model A) and (**B**) absence (model B) of interspecific competition. Dots give biomasses for 500 consecutive years, obtained from simulations. The larger oval depicts the stationary distribution of species biomasses (given by the 90% contour of a bivariate normal distribution approximated with Eq. 2), and the shaded oval gives the joint distribution of annual changes in biomass driven by environmental fluctuations, $\mathbf{E}(t)$. In (A), eigenvectors w_1 and w_2 correspond to eigenvalues λ_1 and λ_2. The variance V_k along each eigenvector w_k equals $U_k + \lambda_k^2 V_k$, as illustrated for w_2. Eigenvectors are not shown for (B) because the stationary distribution is circular. The variance in total biomass is proportional to the variance along w_1 in (A) and the line bisecting the angle between the axes in (B). The variance in total biomass is the same in (A) and (B), even though (A) shows negative covariance between species biomasses.

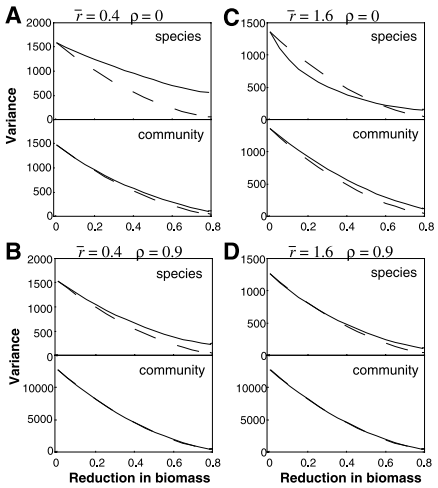

Fig. 2. (**A** through **D**) Species- and community-level variances in biomass (V_n^s and V_n^c) versus proportional reduction in community biomass caused by increasing competition (increasing α). Solid and dashed lines correspond to communities with (model A) and without (model B) interspecific competition, respectively. Each community contains 10 species whose values of r_i and K_i were selected from a normal distribution with standard deviations of 0.1 and 10, respectively. The same sequences of environmental fluctuations $\varepsilon_i(t)$ were used for both models and for all values of α in the same panel. The mean of K_i is 100, the mean of r_i is 0.4 [(A) and (B)] or 1.6 [(C) and (D)], and ρ is 0 [(A) and (C)] and 0.9 [(B) and (D)].

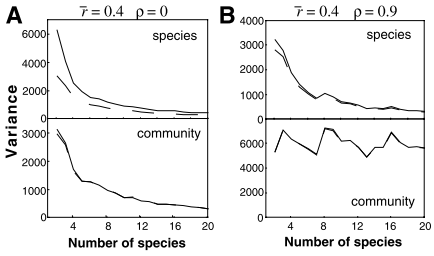

Fig. 3. (**A** and **B**) Species and community-level variances versus the number of species in the communities, n. Solid and dashed lines correspond to communities with (model A) and without (model B) interspecific competition, respectively. Species were added by selecting r_i and K_i from normal distributions with means of 0.4 and 100, respectively, and standard deviations of 0.1 and 10, respectively. Fluctuations with increasing n occur because each added species has randomly selected values of r_i and K_i.

1). These two effects cancel each other, resulting in little net change in community-level variance.

For species-level variances, the effect of interspecific competition depends on the mean intrinsic rates of increase, r_i, as predicted by the analytical results (Fig. 2). It also depends on the correlation in species responses to environmental fluctuations, ρ. As ρ increases, species biomasses tend to vary in synchrony, causing the magnitudes of intra- and interspecific competition to vary in concert. This reduces the contrast between the effects of intra- and interspecific competition on species-level variances (Fig. 2, A versus B and C versus D).

Increasing the number of species n in most cases decreases community-level variances (Fig. 3). To understand why, we consider two communities with n and $n + 1$ species having the same total biomass and no interspecific competition. When $\rho = 0$, species biomasses are not correlated, and the variance in total biomass equals the sum of variances in species biomasses. Variances in total biomass for the two communities are related by $V^c_{n+1} = [n/(n + 1)]V^c_n$. This reduction in community-level variance with increasing n has been called "statistical averaging" (*10*) or the "portfolio effect" (*11*). When species respond similarly to environmental fluctuations ($\rho > 0$), $V^c_{n+1} = [n/(n + 1)]\{(1 + n\rho_s)/[1 + (n - 1)\rho_s]\}V^c_n$, where ρ_s is the correlation between species biomasses. Thus, when ρ, and consequently ρ_s, approaches 1, V^c_{n+1} approaches V^c_n, resulting in no effect of species number on community-level variances. Finally, species number has the same effect in communities with interspecific competition, because the amplification of community-level variances is independent of whether competition is intra- or interspecific (Fig. 2). Thus, increasing n decreases community-level variances by introducing species that respond differently to environmental fluctuations.

Our main result is that interspecific competition and species number have little influence on community-level variances; the variance in total community biomass depends only on how species respond to environmental fluctuations. This contrasts with arguments (*3, 12*) that interspecific competition may decrease community-level variances by driving negative covariances between species abundances. We show that negative covariances are counteracted by increased species-level variances created by interspecific competition.

Consequently, assessing the effect of biodiversity on community variability should emphasize species-environment interactions and differences in species' sensitivities to environmental fluctuations (for example, drought-tolerant species and phosphorus-limited species) (*5, 13*). Competitive interactions are relatively unimportant except through their effects on mean abundances. We have focused on competitive communities, because much current experimental work has addressed competition among plants. Nonetheless, the same results can be shown to hold for more complex models with multiple trophic levels.

References and Notes

1. R. H. MacArthur, *Ecology* **36**, 533 (1955); C. S. Elton, *The Ecology of Invasions by Plants and Animals* (Chapman & Hall, London, 1958); R. Margalef, *Brookhaven Symp. Biol.* **22**, 25 (1969); S. L. Pimm, *Nature* **307**, 321 (1984).
2. R. M. May, *Nature* **238**, 413 (1972); *Stability and Complexity in Model Ecosystems* (Princeton Univ. Press, Princeton, NJ, ed. 2, 1974).
3. D. Tilman and J. A. Downing, *Nature* **367**, 363 (1994); D. Tilman, *Ecology* **77**, 350 (1996).
4. S. L. Pimm, *The Balance of Nature?* (Chicago Univ. Press, Chicago, 1991).
5. S. J. McNaughton, *Am. Nat.* **111**, 515 (1977).
6. A. R. Ives, *Ecol. Monogr.* **65**, 217 (1995); A. R. Ives and V. A. A. Jansen, *Ecology* **79**, 1039 (1998).
7. V_k and U_k are the variances of the projections of $\mathbf{X}(t)$ and $\mathbf{E}(t)$, respectively, onto vector w_k.
8. This follows immediately from the community matrix with diagonal elements $1 - [r/(\alpha + 1)]$ and off-diagonal elements $-r\alpha/[(n - 1)(\alpha + 1)]$.
9. Model A is

$$x_i(t+1) = x_i(t)\exp\left\{\varepsilon_i(t) + r_i\left[1 - \frac{x_i(t) + \frac{\alpha}{n-1}\sum_{j\neq i}^{n} x_j(t)}{K_i}\right]\right\}$$

The competition coefficient α is scaled by $1/(n - 1)$ so that the net strength of interspecific competition is independent of the number of species. Model B is

$$x_i(t+1) = x_i(t)\exp\left\{\varepsilon_i(t) + r_i\left[1 - \frac{x_i(t)}{K_i/(1+\alpha)}\right]\right\}$$

K_i is decremented by $1/(1 + \alpha)$ to produce the same reduction in biomass as model A. For both models, $\varepsilon_i(t)$ values are selected from a multivariate normal distribution with mean 0, variance 0.1, correlation ρ, and no serial correlation.
10. D. F. Doak *et al.*, *Am. Nat.* **151**, 264 (1998).
11. D. Tilman, C. L. Lehman, C. E. Bristow, *ibid.*, p. 277; D. Tilman, *Ecology* **80**, 1455 (1999).
12. J. H. Lawton and V. K. Brown, in *Biodiversity and Ecosystem Function*, E. D. Schulze and H. A. Mooney, Eds. (Springer-Verlag, Berlin, 1993), pp. 255–270; T. M. Frost, S. R. Carpenter, A. R. Ives, T. K. Kratz, in *Linking Species and Ecosystems*, C. G. Jones and J. H. Lawton, Eds. (Chapman & Hall, New York, 1994), pp. 224–239.
13. S. J. McNaughton, *Ecol. Monogr.* **55**, 259 (1985).

14. We thank D. F. Doak, T. M. Frost, S. L. Pimm, N. Schellhorn, D. Tilman, M. G. Turner, and especially S. R. Carpenter for comments and insights. Supported by a grant from NSF.

12 July 1999; accepted 7 September 1999

CFTR Chloride Channel Regulation by an Interdomain Interaction

Anjaparavanda P. Naren,[1]* Estelle Cormet-Boyaka,[1]* Jian Fu,[1] Matteo Villain,[1] J. Edwin Blalock,[1] Michael W. Quick,[1,2] Kevin L. Kirk[1,2]†

The cystic fibrosis gene encodes a chloride channel, CFTR (cystic fibrosis transmembrane conductance regulator), that regulates salt and water transport across epithelial tissues. Phosphorylation of the cytoplasmic regulatory (R) domain by protein kinase A activates CFTR by an unknown mechanism. The amino-terminal cytoplasmic tail of CFTR was found to control protein kinase A–dependent channel gating through a physical interaction with the R domain. This regulatory activity mapped to a cluster of acidic residues in the NH_2-terminal tail; mutating these residues proportionately inhibited R domain binding and CFTR channel function. CFTR activity appears to be governed by an interdomain interaction involving the amino-terminal tail, which is a potential target for physiologic and pharmacologic modulators of this ion channel.

The CFTR chloride channel is implicated in two major human diseases: cystic fibrosis, a genetic disorder that is caused by reduced CFTR function in the lung (*1*), and secretory diarrhea, a fluid and electrolyte disorder that is caused by increased CFTR activity in the gut (*2*). The development of strategies for treating either of these diseases would be facilitated by detailed knowledge of how to activate or inactivate the CFTR channel. The opening and closing of the CFTR channel (gating) is regulated by hydrolysis of adenosine triphosphate (ATP) by one or both of the nucleotide binding domains (NBDs; Fig. 1A)

[1]Department of Physiology and Biophysics, [2]Department of Neurobiology, Gregory Fleming James Cystic Fibrosis Research Center, University of Alabama at Birmingham, Birmingham, AL 35294, USA.

*These authors contributed equally to this report.
†To whom correspondence should be addressed. E-mail: kirk@phybio.bhs.uab.edu